

A New Concept of the Main Rotor for a High-Speed Single-rotor Helicopter.

N.S. Pavlenko
Doctor of Engineering
Deputy Chief Designer

Mil Moscow Helicopter Plant JSC
2 Sokolnichesky Val, Moscow
Russian Federation
e-mail: mvz@mi-helicopter.ru

Key words: High-speed helicopter, stall, retreating blade

Abstract

The paper considers a new concept of the main rotor for a high-speed **single-rotor** helicopter. The essence is to implement a system of local elimination of stall (SLES) on the retreating blade into the main rotor design. This system will allow a helicopter equipped with a conventional main rotor to achieve a cruise speed of 400 km/h without using any additional means of producing propulsive force and a wing. The loads increased due to this fact that are applied to the main rotor hub, mast and blades can be taken by the design. The use of this concept does not lead to any difficult design changes and can be implemented in practice.

Introduction

A single-rotor helicopter is the most effective aircraft in hover. The capability of the helicopter to hover, to take-off and land vertically, as well as to autorotate is the main advantage of the helicopter as an aircraft. However, the main rotor as a propelling device has well known level flight speed limitations thus making it not very effective in level flight conditions; it should be noticed that effectiveness decreases with speed. A longstanding experience of attempts to design VTOL aircraft of different types, such as rotary wing, tilt rotor aircraft, as well as aircraft using the ABC concept, aircraft with rotors stopped in flight and others has shown that at present helicopters of conventional concepts are the most optimal and feasible. When passing to compound aircraft the main helicopter qualities are either lost or deteriorate unacceptably (thus, for instance, the autorotation capability can be lost). But

due to a high complexity of the design, development and serial production of specimens require huge financing. At the same time, the potentialities of conventional helicopter concepts, including that of the single-rotor one, are not fully unveiled. This concerns mainly the helicopter maximum speed increase.

The single-rotor helicopter maximum speed is limited to a number of factors: retreating blade stall, approach of the advancing blade tip local flow velocities to the M value equal to 1 leading to appearance of shock waves, limitations due to static and fatigue strength of the rotor system units, etc. However, the retreating blade stall is the first and main obstacle connected with aerodynamics and dynamics of the main rotor in the oblique flow in level flight conditions. To a higher degree it concerns main rotors whose blades are hinged to the hub or attached to it by means of a flexible member with low flapwise stiffness for bearingless main rotors (BMR).

1. Retreating Blade Stall

As is known, the blade member thrust will change with azimuth in level flight due to the non-uniform distribution of the velocity field along the rotor disc. The thrust on the advancing blade will increase while it will decrease on the retreating blade. The balance of the roll moment moving from the advancing blade to the retreating blade (to the right, if the main rotor turns clockwise when looked from above) occurs due to the balance of the helicopter and the blade flapping motion where additional downwash on the airfoil is produced. The flapping motion results in such a redistribution of

actual blade airfoil angles of attack in azimuth that these angles of attack at azimuth $\psi=\pi/2$ decrease, while they significantly increase at azimuth $\psi=3/2*\pi$. As soon as the level flight speed reaches the critical value a stall occurs at $\psi=3/2*\pi$.

It is not allowed to enter the stall area because of a sharp growth of loads applied to the rotor and control systems, helicopter vibration growth and so on and so forth. Fig. 1 shows that the blade section angles of attack are small at azimuth in the area of $\psi=\pi/2$ where the blade section flow velocity is the greatest as the blade is underloaded, and at azimuth close to $\psi=3/2*\pi$ the angles of attack reach the critical values where a stall occurs.

In addition, this redistribution of the aerodynamic force along the rotor disc results in a reduction of the total thrust and even more of the propulsive force with flight speed. Due to these reasons it is extremely difficult for the single-rotor helicopter to achieve level flight speeds of 320-350 km/h without using some additional means (such as a wing, propellers). If, for example, the advancing blade angles of attack ($\psi=\pi/2$) could be increased and the retreating blade angles of attack ($\psi=3/2*\pi$) could be decreased this would result, first, in the elimination of the stall, and, second, in full loading of the advancing blade, i.e. the most effective part of the disc having the greatest flow velocity. This would lead to a significant improvement of the main rotor aerodynamic characteristics and a significant increase in the maximum flight speed and altitude. But this redistribution of the angles of attack would result in a roll moment. Therefore the solution lies in the search of means capable of trimming this helicopter roll moment.

Many papers, such as [1], [2], [3], [4], [5], [6], [7], [8], in this or that degree, consider additional means trimming the roll moment not connected to the helicopter main rotor. They are as follows: a one-side wing, a shift of the helicopter CG relative the main rotor vertical axis as well as auxiliary means producing propulsive force (propellers or propulsion engines) unloading the main rotor.

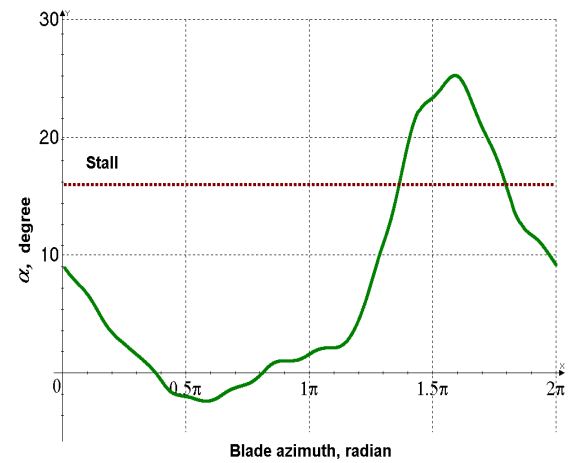


Fig. 1. Blade tip angles of attack versus azimuth

Tilt rotor aircraft and multicopter helicopters where the problem of balancing the roll moment does not exist or can be solved much easier, are not as widely used as the single-rotor helicopters because of their design sophistication.

In the 1970s the Sikorsky Aircraft Division started to work at developing a high-speed helicopter using the ABC concept for a twin coaxial rigid rotor. In this case the roll moments produced at the upper and lower rotors are mutually balanced.

However, high levels of loads applied to the advancing blade in this case due to the ABC concept implementation due to very significant roll moments opposite in sign occurring in the rotors in combination with the complexity inherent in the coaxial rotor design did not allow this concept to be improved to the level providing it mass production.

The XH-59A helicopter in 1973 built by using this concept attained a speed of 236 knots (~437 km/h) in level flight in 1980 after many years of refinement [7], [8]. But a high level of rotor and mast loading, as well as problems connected with the structure, cost effectiveness, load ratio and others, made it impossible to continue working at this helicopter [8].

In 2005 Sikorsky Aircraft Division announced initiation of a program aimed at development of a flight demonstrator designed X2 equipped with contra-rotating rigid rotors and a pusher propeller installed in the tail. It was stated that the X2 design speed would be 250 knots (~462 km/h). The

first flight was planned for the end of 2006, but it was postponed till the end of 2007 [9].

2. Stall Local Elimination System (SLES)

The paper considers a method making it possible to cope effectively with the problem of balancing the roll moment occurring on the single-rotor helicopter main rotor at high speeds when the azimuth aerodynamic loading is redistributed which is necessary to reduce the retreating blade angles of attack below the critical ones. It involves a stall local elimination system (SLES). The offered solution means the introduction of a system enabling to transform the hub flexural-kinematic parameters into an optimal version in control inputs.

It can be achieved by changing the flapwise flexural stiffness of the hub sleeves or by limiting angular movements in the flapping hinge within the given azimuth sector. To do this, the main rotor hub (Fig. 3-5) is equipped with means deactivating the flapping hinges within the given azimuth sector that are made as hydraulic locks controlled via slide valves.

The installation of hydraulic locks limiting angular movements of the blades in the flapping hinges gives the hinged hub properties of a rigid rotor within the given azimuth sector.

Let us consider the helicopter main rotor disc cross-section in a steady level flight condition (Fig. 2). When the hydraulic lock in the azimuth right sector is activated the root acquires increased rigidity which equals a change in the value of the flapping hinge equivalent offset when the blade passes this azimuth sector. It results in an additional roll moment M_{r2} directed towards the advancing blade that will balance the roll moment M_{r1} produced by cyclic control to offload the right portion of the disc ($\psi = 3/2 * \pi$) and to increase aerodynamic loading in the left portion ($\psi = \pi/2$). Thus, this design of the hub enables to get the required roll moments necessary to balance the roll moments produced by cyclic control; they serve to redistribute the azimuth angles of attack of the blade sections in such a manner that enables to eliminate the retreating blade stall, and, therefore, to increase the helicopter flight speed.

$$M_{kp1} = M_{kp2}$$

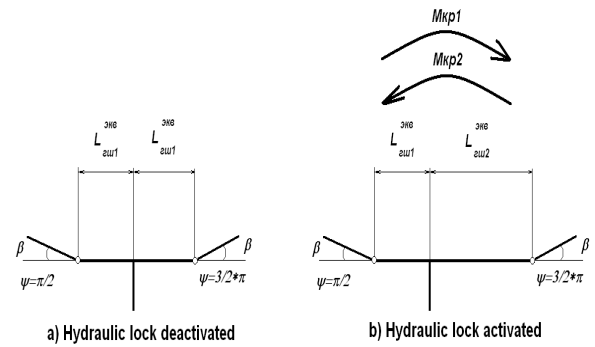


Fig. 2

3. SLES Concept Implementation and Principle of its Operation

This particular concept for a two-bladed rotor and somewhat different application was first described in paper [10].

Fig.3 shows the offered concept implemented into a helicopter five-bladed hinged main rotor. The hub has boss 1 rigidly fixed to main rotor mast 2. Blade 3 is fixed to boss 1 with the help of flapping hinge 4, drag hinge 5 and feathering hinge 6. In addition, the hub has means deactivating the flapping hinges made as hydraulic locks 7 with electromagnets 8 and slide valves 9. The hydraulic lock case has hinge bearing 10 located on the hub boss, and piston rod 11 is connected to bearing 12 located on the flapping hinge via the hinge unit.

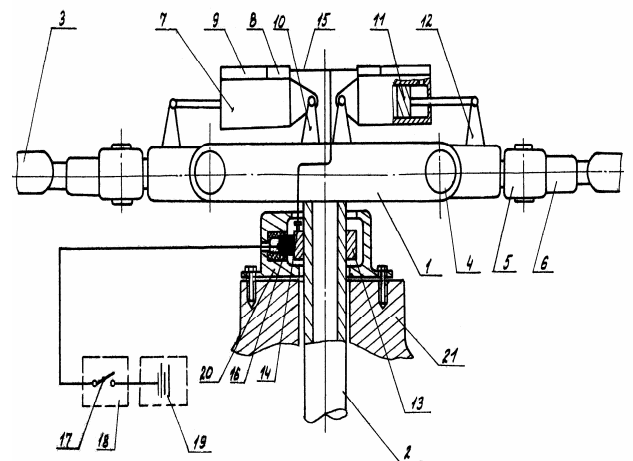


Fig. 3. General Arrangement Drawing of a Five-bladed Main Rotor

Ring 13 is fixed to the main rotor mast and rotates with the latter. The ring is connected to the electromagnet coils via terminal 14 and electric wiring 15. The ring is connected to switch 17 located in cockpit control panel

18 and power source 19 via sliding contact 16 and electric wires. The sliding contact is placed inside slip ring case 20 which is installed on main gearbox case 21. The slide valve unit is in the upper part of the hydraulic lock case; it consists of sliding valve 22 (Fig. 4) with grooves 23, spring 24 and plate 25.

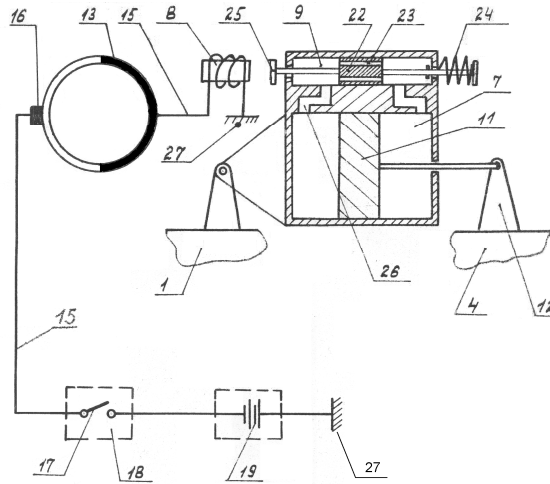


Fig. 4. Simplified Diagram of the Device Deactivating Flapping Hinges

Grooves 26 connect the sliding valve and hydraulic lock cavities. The negative poles of the power source electromagnet coils are connected with “mass” 27. Rings 13 provide locking of the flapping hinges at half the azimuth of each blade leaving them free in the remaining part. Therefore half of their surface contacting the sliding contacts is covered with an insulation material (Shown as black in the figure). Switch 13 initiates the activation of the operational modes of the above rings. The hub operates in the following sequence (see Fig. 4). The electric circuit is open when switch 17 is off. The current is not supplied to the coil of electromagnet 8, and spring 24 uncoiling moves slide valve 22 to the position shown in Fig. 4. When piston 11 moves in the cylinder of hydraulic lock 7, the liquid along grooves in the slide valve unit 26 and slide valve 23 runs freely from one cavity of the cylinder into the other not producing any drag for the piston. Hydraulic lock 7 is in the “off” position and the flapping hinges operate as they do in the hinged hub. Prior to transition to a flight speed exceeding 300 km/h, the pilot displaces switch 17 to the “on” position. The current starts running from power source 19 along electric wires

15 via sliding contact 16 to ring 13 rotating with the main rotor mast and then it passes through the coil of electromagnet 8 to “mass” 27. The electromagnet attracts plate 25, and, compressing spring 24, displaces slide valve 22 to the extreme left position. The slide valve shuts off left groove 26, thus separating the hydraulic cylinder cavities. As any liquid is incompressible, piston 11 stops. The flapping hinge is locked, and the hub operates as if it were a part of a “rigid” rotor.

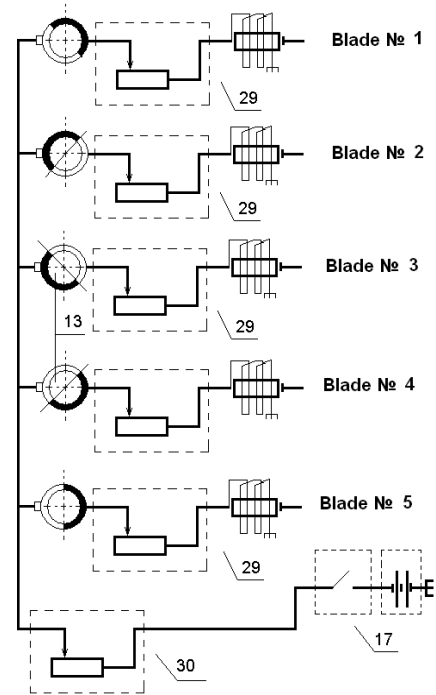


Fig. 5. Diagram of Activating Lock Rings of Flapping Hinges at Some Azimuth for a Five-bladed Main Rotor

Fig. 5 shows an electric diagram for parallel switching of rings 13 for a five-bladed main rotor. Rings 13 are placed on the main rotor mast so that the isolated half-surface of each of them is shifted by $\Delta \psi = 2\pi/5$ relative to the isolated half-surface of the neighbouring rings. The circuit of each blade during one turn of the main rotor turns out to be open and closed once. Therefore, the flapping hinge of each blade is once locked in the azimuth sector from $\psi = 2$ to $\psi = \pi/2\pi$. Units 29 are designed for a smooth change in the hub sleeve stiffness providing the transition of blades from a hinged connection to a rigid one.*

* The electromechanical system of rings 13 can be replaced by an electronic unit.

Unit 30 is designed for a smooth transition of the main rotor to the SLES mode. In this design there are no intricate members difficult in manufacturing.

Moreover, the system is based on similar components used in actual operation such as slip rings, and drag hinge hydraulic dampers that can be combined with slight changes in the available hubs, both three-hinged and those having hinges with elastomeric bearings.

4. Prediction Method

To determine the main rotor aerodynamic characteristics and to make calculations for the main rotor strength, the method presented in papers [11], [12], [13], [14] is used. The method describes small oscillations of the turning main rotor by a system of quartic differential equations in partial derivatives.

$$L[q(r,t)] = F \quad (2)$$

Here L is the system operator including three equations in partial derivatives relative to unknown functions $q(r, t)$ and required boundary conditions

$$q(r, t) = \begin{pmatrix} x \\ y \\ \varphi \end{pmatrix} \quad (3)$$

where

- q column matrix of generalized coordinates
- x blade chordwise displacement (deformation)
- y blade displacement (deformation) in the plane containing the rotor axis of rotation
- φ blade torsional displacement and deformation relative to its longitudinal axis
- F aerodynamic load vector

The blade and hub root is described by a stiffness matrix in which each element is a force directed towards the q_k force factor at a single displacement towards q_n :

$$C = \begin{pmatrix} C_{XX} & C_{XX'} & C_{XY} & C_{XY'} & C_{X\Phi} \\ C_{X'X} & C_{X'X'} & C_{X'Y} & C_{X'Y'} & C_{X'\Phi} \\ C_{YX} & C_{YX'} & C_{YY} & C_{YY'} & C_{Y\Phi} \\ C_{Y'X} & C_{Y'X'} & C_{Y'Y} & C_{Y'Y'} & C_{Y'\Phi} \\ C_{\Phi X} & C_{\Phi X'} & C_{\Phi Y} & C_{\Phi Y'} & C_{\Phi\Phi} \end{pmatrix} \quad (4)$$

The centrifugal and lateral forces, as well as the bending moment acting in the blade cross

section and transmitted to the hub are considered as force factors. The solution of the equation system is presented as an expansion in a series in their normal modes. Having determined the frequency and mode of natural oscillations, coefficients usually called as strain coefficients remain unknown in the solution. These coefficients are determined after applying the Galerkin method to the system of differential equations by numerical integration.

The aerodynamic forces F included in the right-hand part of the equation system are calculated by using lift, drag and torque coefficients (C_y, C_x, m_2 respectively) versus the blade airfoil angle of attack and M number obtained from wind tunnel testing.

The introduction of the azimuth variable springing C in the hub flapping hinges is made through the matrix coefficient (4)

$$C_{y,y'} = C f(\psi) \quad (5)$$

5. Results of Calculations Obtained

5.1. Helicopter Configuration Versions

In investigating possible application of the SLES system the following configurations of a single-rotor helicopter were considered:

I. A single-rotor helicopter of the Mi-8 type equipped with a five-bladed main rotor with the Mi-38 blades. This configuration was used as a test-bed for exploring the Mi-38 rotor system.

The blade without swept tip were considered in this version of calculations.

II. This version differs from the previous one by a lighter takeoff weight (by 1,500 kgf) and by reduced helicopter parasite drag.

5.2. Results of Calculations Made for Version I

To provide a smooth transition of blades from the left-hand to the right hand sector of the main rotor disc, a smooth change in the flapping hinge stiffness that can structurally be provided by device 29 (Fig. 5) was assumed. Fig. 6 shows the law of the azimuth stiffness variation (5). The above stiffness result in changes in the blade resonance diagram, whose natural

frequencies of separate tones can come to resonances with harmonics of the aerodynamic load.

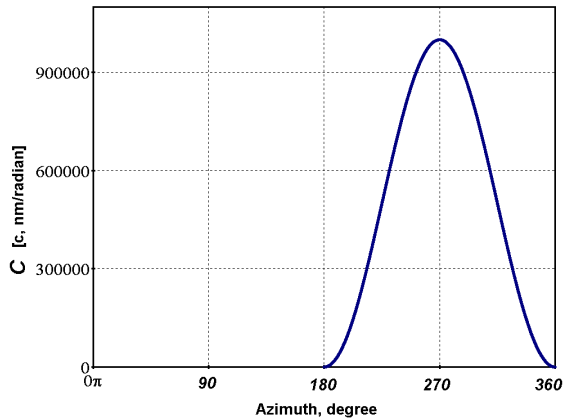


Fig. 6. Law of Variation of Stiffness versus Azimuth

Fig. 7 shows the above changes versus the flapping hinge stiffness logarithm. The n1-n5 lines as well as solid lines in the diagram show numbers of the harmonics of the aerodynamic load and p1-p8 denote blade natural frequencies.

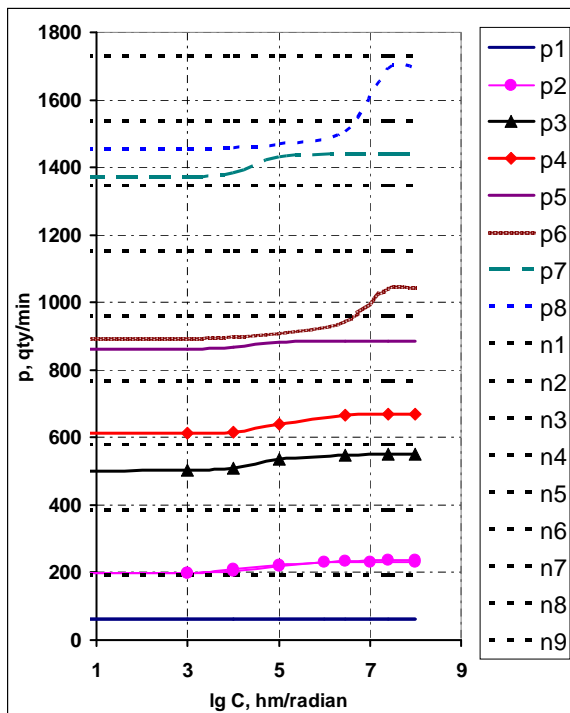


Fig. 7. Blade Natural Frequencies versus Flapping Hinge Stiffness

As can be seen from the diagrams, the 2nd and 3rd flapwise bending modes (p6 and p8 in the diagram) for the flapping hinge stiffness slightly exceeding $C=10^6$ n·m/rad are in resonance with the 5th and 8th harmonics of the aerodynamic loads when the blade passes into the disc right-hand

sector. To preclude resonances, the values of the maximum stiffness $C=10^6$ n·m/rad was taken. Fig. 8 shows the blade tip section angles of attack ($r=0.98$) versus azimuth for different values of the flapping hinge stiffness (C).

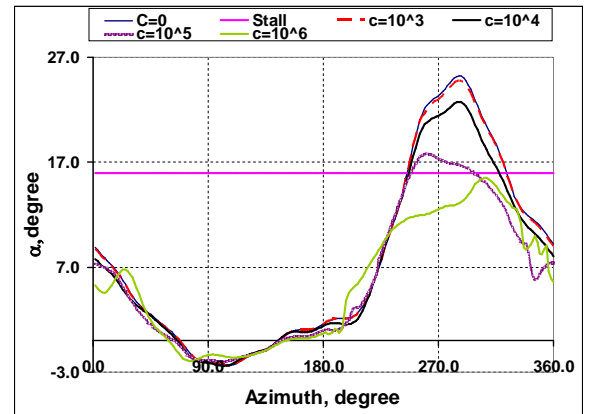


Fig. 8. Angle of Attack at $r=0.98$

As can be seen from the diagrams, the retreating blade is in the area of a deep stall for the hinged rotor (stiffness $C=0$) at a speed of 330 km/h. As soon as stiffness is introduced into the flapping hinge by means of the SLES system, the maximum angles of attack reduce and the retreating blade leaves the stall area at $C=10^6$ n·m/rad. For the given stiffness C the hinged rotor turns into a rigid one in the right-side of azimuth.

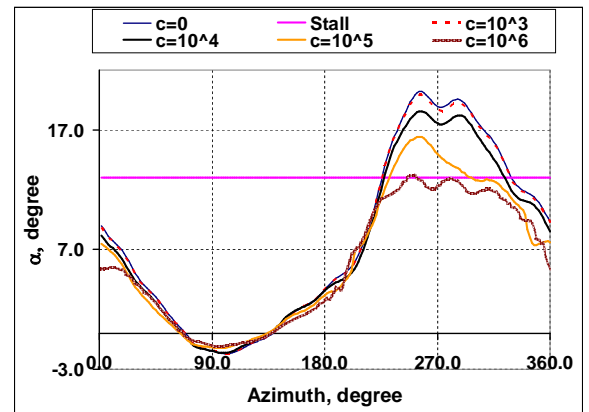


Fig. 9. Angle of Attack at $r=0.91$

Fig. 9 shows similar diagrams for the relative radius $r=0.91$ having the main TsAGI-3 high-lift airfoil. This part of the blade also leaves the stall area. As can also be seen from the comparison of the two diagrams, the blade tip (with greater relative radii) is deeper in the stall area.

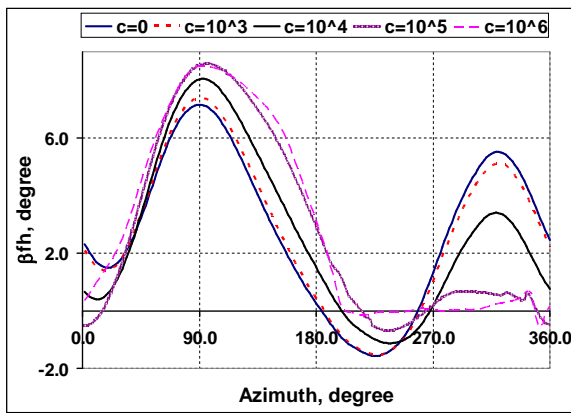


Fig. 10. Blade Flapping Angle in Flapping Hinge

The comparison of flapping motion of the blades for the hinged rotor and that operating with the SLES system (Fig.10) shows a drastic reduction of flapping motion due to the SLES system.

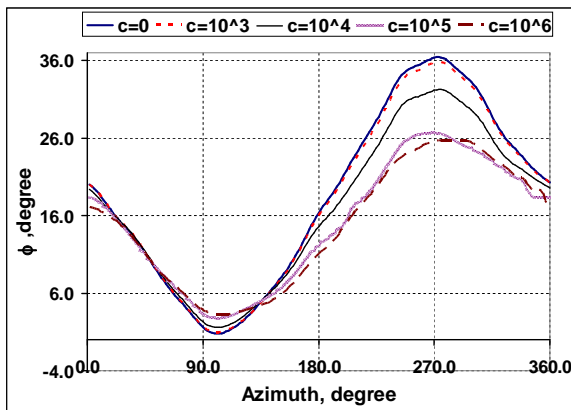


Fig. 11. Blade Section Angle of Setting

At the same time the required blade settings also decrease (Fig. 11). Calculations of the rotor flapwise bending moments have shown that the use of the SLES system results in an increase in loads (Figs. 12, 13).

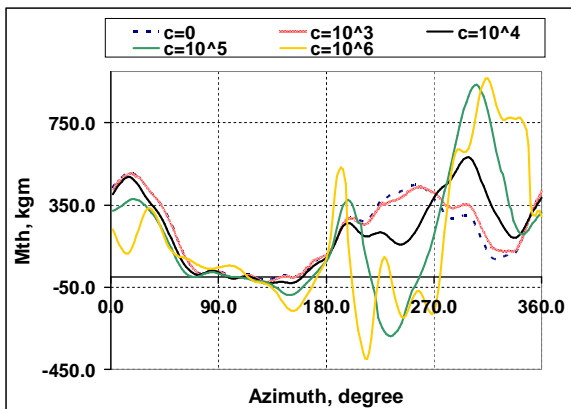


Fig. 12. Flapwise Bending Moment in Blade Root

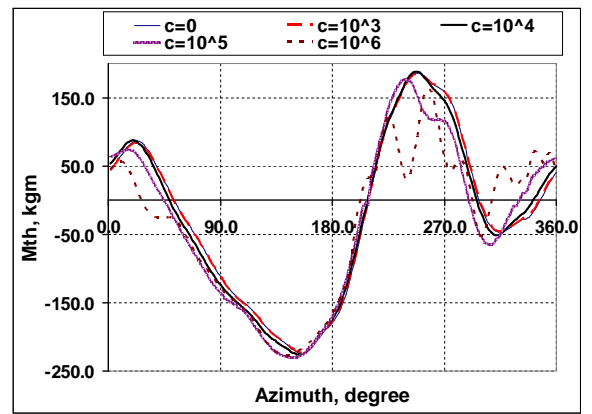


Fig. 13. Blade Flapwise Bending Moment at $r=0.54$

It should be noted that this increase in the middle of the blade ($r=0.54$) is slight while it is more significant in the root which should be for the rigid rotor and it can be taken by the appropriate reinforcement of the hub.

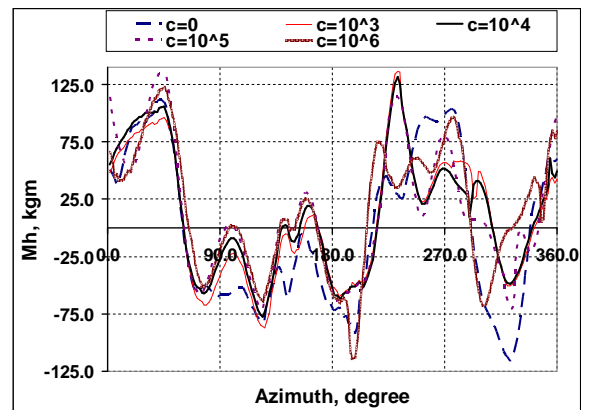


Fig. 14. Hinge Moment

The hinge moments and, therefore, control loads have changed insignificant both in the magnitude and in harmonic content (Fig.14).

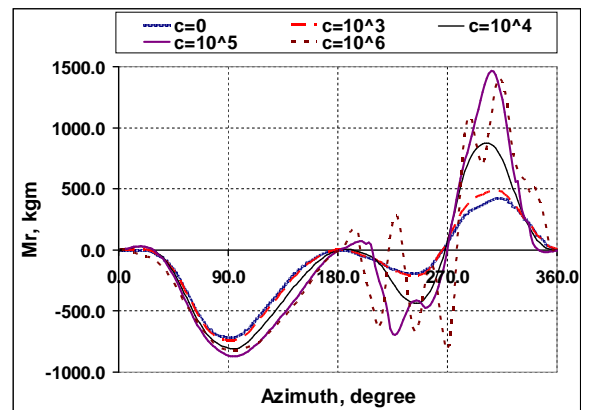


Fig. 15. Roll Moment Produced by One Blade

Fig. 15 shows the roll moment transmitted to the hub one blade versus azimuth. It can be seen the use of the SLES system produces a

significant lateral moment acting from the side of the retreating blade toward the advancing one which, as it was stated. This enables the roll moment resulted due to the redistribution of the aerodynamic load along the rotor disc due to cyclic control to be balanced and to put off the retreating blade stall.

5.3 Results of Calculations Made for Version II

Version II is a helicopter configuration made on the basis of the Mi-8 (Version I) but incorporating a number of changes contributing to higher helicopter speeds and the application of the SLES system. They include: a reduction of the helicopter takeoff weight up by 1,500 kgf maintaining the same rotor parameters, a decrease of the helicopter drag by making the fuselage cleaner, use of retractable landing gear, main rotor hub fairing, etc.

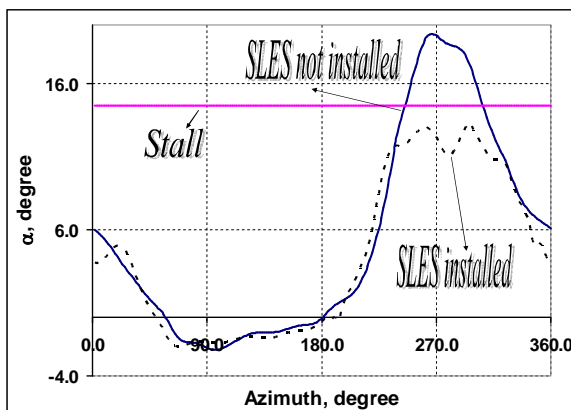


Fig. 16. Angle of Attack at $r=0.98$

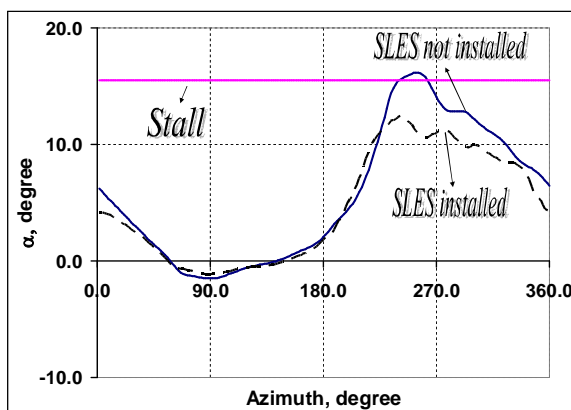


Fig. 17. Angle of Attack at $r=0.91$

Figs. 16-17 present the results obtained from calculations of changes in azimuth angles of attack of the blade tip section and the section from which the main lift airfoil runs required for speeds of 360 km/h..

It can be seen from the diagrams that the helicopter can attain a level flight speed of 360 km/h due to the retreating blade stall elimination. When the speed is increased up to 400 km/h, in this helicopter and rotor system configuration a stall occurs at the blade tip and in the section from which the main lift airfoil runs (Figs. 18, 19). These diagrams do not present curves for a speed of 400 km/h without the SLES system as the angles of attack for the retreating blade azimuth become very great.

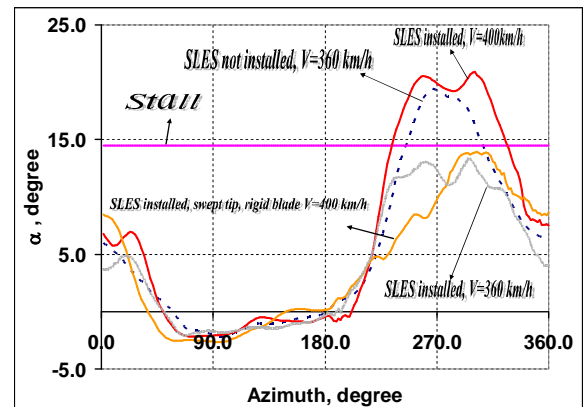


Fig. 18. Angle of Attack at $r=0.98$

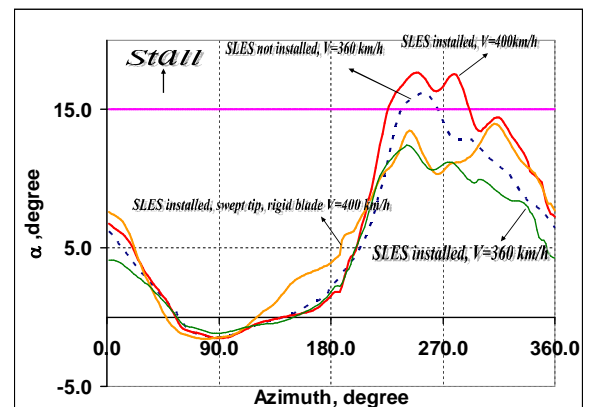


Fig. 19. Angle of Attack at $r=0.91$

Further increase in flight speeds becomes possible only when some changes into the rotor system are introduced. The first of them is to increase the blade flapwise stiffness. This makes it possible to increase additionally the value of the flapping hinge equivalent offset in the retreating blade (L_{fh}^{equiv} , see Fig. 2) with the application of the SLES system, and thus to increase its efficiency. Besides, a swept blade tip was introduced. This enables the blade to leave the stall area (Figs. 18, 19) at a speed 400 km/h.

5.4 Further Prospects for Single-rotor Helicopters to Increase Speed in Level Flight

To increase the single-rotor helicopter speed in level flight exceeding 400 km/h (up to 500 km/h and higher), it is necessary to use additional means to develop propulsive force alongside with the SLES system. From our point of view, these means can be propellers. In this case the main rotor will produce lift only at high flight speeds, therefore the main rotor angle of attack will equal zero. Besides, at speeds exceeding 400 km/h, the flow around the advancing blade tip approaches the speed of sound, limitations related to compressibility and shock waves arise. To put off the above limitations caused by higher speeds, it is necessary to reduce the blade tip speed up to $\omega R=180$ m/s. Swept blade tips are an additional means increasing compressibility margins. It should be noted that, to fly at speeds exceeding 400 km/h, the aerodynamic configuration of the main rotor blade should essentially be changed. Besides, it is necessary to reduce further the helicopter parasite drag.

Final Remarks

1. A method making it possible to put off the retreating blade stall on the single-rotor helicopter and its structural implementation is offered; it leads to a redistribution of the rotor disc aerodynamic load, and changes in the blade root stiffness properties make it possible to compensate the roll moment produced on the single-rotor helicopter main rotor due to its overbalance.
2. Proceeding from the results obtained from the calculations, it has been proven that a single-rotor helicopter can attain level speeds of up to 400 km/h without any additional means producing propulsive force and a wing.
3. This particular configuration contains no sophisticated members difficult for manufacturing. Moreover, the system is based on similar members being in actual operation: a slip ring, and drag hinge hydraulic damper. They can be arranged with the existing main rotor hinged hubs, as well as hubs equipped with elastomeric

bearings and bearingless hubs by introducing insignificant changes into them.

4. One of the advantages of the SLES system is that it can be activated only at a maximum speed. It means that at takeoff, landing, hover, acceleration, deceleration and low speed flight conditions it can be deactivated thus saving the lifetime of the helicopter rotor system.

References

1. Payne P.R. Helicopter Dynamics and Aerodynamics (translation from English). M., Oborongiz, 1963
2. S.Yu. Esaulov, O.P. Bakhov, I.S. Dmitriev. Helicopter as an Object of Control. M., Mashinostroyenie, 1977
3. A.Yu. Liss. Investigation of Some Methods Improving Main Rotor Characteristics at High Flight Speeds. Moscow Helicopter Plant Technical Report No. 4, M., 1968
4. A.V. Nekrasov. Dynamics, Strength and Aerodynamics of the "Rigid" Main Rotor. Moscow Helicopter Plant Technical Report, M., 1968
5. E.I. Ruzhitsky. World Records of Helicopters. Vertolet Publishing House, 2005
6. Palgino V. Forward Flight Performance of a Coaxial Rigid Rotor. Proceedings of 17th Forum of American Helicopter Society, 1971
7. Raymond L. Robb. Hybrid Helicopters: Compounding the Quest for Speed. Vertiflite, Summer 2006
8. Ray Prouty. Another Look at the Advancing Blade Concept. Vertiflite, Summer 2006
9. John Crott. X2 Marks the Spot for Radical Rotor Designs. Flight International, 12-18 June, 2007
10. N.S. Pavlenko, V.M. Pchelkin. Helicopter Main Rotor Head. Certificate of Authorship No. 1658538, 1991
11. N.S. Pavlenko. Natural Bending and Torsional Oscillations of the Main Rotor Blade with a Swept Tip. Numerical and Experimental Methods Used for Investigation of Aircraft Structural Strength. M., MAI, 1989
12. N.S. Pavlenko, A.Yu. Barinov. Selection of Design Parameters for Elastic Components in Designing Helicopter Semi-rigid Rotor Heads. Proceedings of 1st Forum of Russian Helicopter Society and Yuryevsky Readings. M., 1995
13. Pavlenko N.S., Barinov A.Yu. Analysis of Torsion Moments Produced in Main Rotor Blades and Results Obtained. 21st European Rotorcraft Forum. St. Petersburg, Russia, 1995
14. Dr. Pavlenko N.S., Barinov A.Yu. Procedures Used to Ensure Sufficient Strength and Damping in Helicopter Bearingless Rotors. 22nd European Rotorcraft Forum, Brighton, UK, 1996